CMLS, Cell. Mol. Life Sci. 58 (2001) 298–306
1420-682X/01/020298-09 $ 1.50 + 0.20/0

CMLS Cellular and Molecular Life Sciences

Research Article

Analysis of nuclear apoptotic process in a cell-free system

Y. Zhao, M. Wu, Y. Shen and Z. Zhai*

College of Life Sciences, Peking University, Beijing 100871 (P. R. China), Fax + 86 10 62751526,
e-mail: zhaizh@plum.lsc.pku.edu.cn

Received 29 September 2000; received after revision 10 December 2000; accepted 13 December 2000

Abstract. We report an analysis of the apoptotic process of mouse liver nuclei induced in a cell-free carrot cytosol system by cytochrome c. Typical characteristics of apoptosis were observed, such as chromatin condensation, margination, apoptotic bodies and DNA ladders. Furthermore, transmission and scanning electron microscope analysis of the apoptotic nuclei detected chromatin-free nuclear vesicles before apoptotic bodies appeared at a comparatively late phase. When AC-YVAD-CHO, an inhibitor of caspase 6, was introduced into the system, these vesicles and apoptotic bodies disappeared completely within our study sections. We confirmed the results using whole-mount electron microscopy, and found that although the nuclear lamina was destroyed early, the nuclear matrix largely remained intact during the course of apoptosis. The nuclear matrix played an important role in maintaining the integrity of apoptotic cells and connecting the apoptotic bodies and apoptotic nucleus.

Key words. Apoptosis; cell-free system; electron microscope; lamina; nucleus.

Apoptosis is one form of cell death that is well controlled by a genetic program which may be activated by inner or exterior signals. Apoptosis is vital for both normal development and the maintenance of many tissues in multicellular organisms [1]. Cells undergoing apoptosis show characteristic morphological features including chromatin condensation, margination, the formation of apoptotic bodies, and DNA ladders [2, 3]. Earlier studies indicated that the morphological changes were due to a series of biochemical reactions in which caspases play key roles [4, 5]. Lamin degradation by activated caspase 6 directly results in the nuclear morphological changes seen in the process of apoptosis [6]. In a living cell, the lamina is formed by three kinds of lamins, lamin A, B, and C. They form a network under the nuclear membrane and contribute to the normal structure of the nucleus by cooperating with the nuclear matrix [7]. For example, chromosomes are connected with the lamina through telomeres and evolve in the space structure [8–11]. The degradation of lamin proteins, which can be inhibited by Ac-YVAD-CHO, parallels the event of DNA fragmentation during the execution of apoptosis [12].

The specific apoptotic morphological changes are hallmarks of apoptosis [2, 3, 13]. To understand the structural basis of apoptotic morphology, we characterized nuclear apoptosis in a cell-free system, a useful experimental system for research into the apoptotic mechanism [4, 14–18]. We have developed a carrot cytosol cell-free system named CS-100 [17–19]. Cytochrome c is responsible for mediating the apoptotic downstream pathway from mitochondria [4, 20, 21]. We have shown that cytochrome c can drive both carrot nuclei and mouse nuclei into the apoptotic process in the CS-100 system [17, 18]. This suggests that plant and animal cells may share a similar apoptotic signal pathway [18]. In

* Corresponding author.

the CS-100 induction system, nuclear lamins underwent typical degradation during apoptosis of nuclei [18]. However, we still do not know the details about the changes in apoptotic nuclei and the function of lamins during apoptosis. Using transmission (TEM) and scanning (SEM) electron microscopy, in the work described here, we found that the formation of apoptotic bodies was preceded by the appearance of chromatin-free nuclear vesicles. Furthermore, Ac-YVAD-CHO could inhibit the formation of chromatin-free nuclear vesicles and, moreover, specific degradation of DNA and lamins processed synchronously during the apoptotic process of nuclei. These results demonstrated that during the changes in apoptotic nuclei, the specific degradation of lamins and chromatins are parallel and synchronous events, both of which lead to the structural formation of apoptotic bodies. In addition, we showed that part of the nuclear matrix persists during the process of apoptosis, whereas the lamina system is destroyed. The nuclear matrix connects the apoptotic bodies and apoptotic nucleus, and is the structural foundation of apoptotic bodies.

Materials and methods

Preparation of interphase nuclei of mouse liver. The preparation and purification of interphase mouse liver nuclei was performed following the method of Blobel and Potter [22]. The nuclei were suspended in nuclei storage buffer (10 mmol/l PIPES, 80 mmol/l KCl, 20 mmol/l NaCl, 250 mmol/l sucrose, 5 mmol/l EGTA, 0.5 mmol/l spermidine, 0.2 mmol/l spermine, 50% glycerol) after being centrifuged at 124,000 g (Beckman TLS-55) and counted before storage in a freezer at -196.

Preparation of carrot protoplasts and cytosol extraction CS-100. About 5 g suspension of carrot cells (gross weight), cultured for 5–7 days, was added into 10 ml enzymatic buffer [2% (w/v) cellulase, 0.5% macerozyme, 5 mmol/l MES, 6.8 mmol/l $CaCl_2$ 11 mmol/l KH_2PO_4, 0.6 mol/l mannitol, 0.4% PVP, pH 5.8], treated with an orbiting speed of 50–80 rpm in the dark at 28 °C for 2 h. After being filtered through a no. 200 nylon mesh, the protoplasts were harvested by centrifugation at 120 g for 5 min. After the protoplast sediment had been resuspended in the 0.6 mol/l sucrose buffer, the purified protoplasts, which located in the upper layer, were collected by centrifugation at 120 g for 5 min. Buffer A (20 mmol/l Hepes-KOH, 10 mmol/l KCl, 1.5 mmol/l $MgCl_2$, 1 mmol/l EDTA, 1 mmol/l EGTA, 1 mmol/l DTT) [4] was added to the purified protoplasts, which were then homogenized. Aprotinin, PMSF, and leupeptinin were added to the buffer at final concentrations of 6 mg/ml, 0.1 mmol/l, and 8 mg/ml, respectively. After centrifugation at 100,000 g (Beckman TLS-55) at 4 °C for 2 h, the soluble cytosol was collected and named cytosol CS-100 [17].

Induction of apoptosis and detection of apoptotic nuclei. When cytochrome c was added to the CS-100 cell-free system at a concentration of 2 μmol/l, it transformed this cytosol cocktail into a highly efficient apoptosis induction cell-free system. About 1×10^5 mouse liver nuclei were introduced into 50 μl CS-100 and the system was incubated at 23 °C. To observe the morphological changes of apoptotic nuclei, samples were taken at different times, mixed with 2.5% (v/v) glutaraldehyde and 0.5 μg/ml DAPI for fixation and staining. Slides were sealed with glycerol and PBS (1:1, v/v), and then observed under a fluorescent microscope (Leica DMRB). Photographs were taken at the same time.

Detection of apoptotic nuclei DNA. Samples induced for 0.5, 1, 2, and 4 h were suspended in 10 vol of buffer D (100 mmol/l Tris-HCl, pH 8.0, 5 mmol/l EDTA, 0.2 mol/l NaCl, 0.4% SDS, 0.2 mg/ml proteinase K) [4], incubated overnight at 37 °C, then extracted with 1:1 phenol:chloroform, and precipitated by 2 vol of ethanol. DNA extracts were electrophoresed in 1.2% agarose gels in TBE buffer. DNA was visualized by ethidium bromide staining, observed, and photographed.

Preparation of samples for TEM. For inducing apoptosis, about 1×10^5 nuclei were added into 50 μl of the CS-100 induction system and incubated at 23 °C. Samples were taken consecutively at time intervals of 30 min. For testing the influence of Ac-YVAD-CHO, 5 μmol/l Ac-YVAD-CHO (Sigma) was added into the cell-free induction system and incubated at 23 °C for 1 h. Then all the samples were fixed at 4 °C for 1 h in a final concentration of 0.5% (v/v) glutaraldehyde. The sediments were collected at 500 g for 3 min, then fixed at 4 °C for 1 h in a final concentration of 1% OsO_4. After dehydration in a graded series of ethanol and acetone (15 min each) and embedding in Epon 812, the samples were cut into silver-gray or white sections using a Leica Ultracut R cutter. After staining with uranyl acetate and lead citrate, the sections with apoptotic nuclei were observed and pictures taken under the JEM-1010 transmission electron microscope.

Preparation of samples for SEM. Sample fixation followed the methodology described above. After dehydration in a graded series of ethanol, the samples were then treated with a graded series of mixed solutions of ethanol and iso-amyl acetate (2:1, 1:1, 15 min each), and then with pure iso-amyl acetate twice (15 min each). After critical point drying in CO_2, the apoptotic nuclei samples were observed, and pictures taken under an AMRAY 1910FE scanning electron microscope.

Preparation of samples for whole mount electron microscope. Apoptosis-inducing samples were taken consecutively at intervals of 30 min, and the sample with 5

μmol/l Ac-YVAD-CHO was taken after 2 h incubation. All samples were then spotted on the copper net with polylysine and adsorbed at room temperature for 30 min. After three washes in PBS (pH 7.2, 5 min each), 20 μl CSK buffer (10 mmol/l PIPES, 100 mmol/l KCl, 300 mmol/l sucrose, 3 mmol/l $MgCl_2$, 1 mmol/l EGTA, 1.2 mmol/l PMSF, 1% Triton X-100, pH 6.8) was dropped onto each copper net and incubated for 10 min. CSK buffer was then removed and 20 μl RSB-Magik buffer (42.5 mmol/l Tris-HCl, 8.5 mmol/l NaCl, 2.6 mmol/l $MgCl_2 \cdot 6H_2O$, 1.2 mmol/l PMSF, 1% Tween-40, 0.5% sodium deoxycholate, pH 8.3) was dropped onto the copper net. Ten minutes later, the RSB-Magik buffer was removed and the copper net was washed three times with PBS (pH 7.2, 5 min each). The copper net, to which the apoptotic nuclei were adsorbed, was digested with DNase I (100 mg/ml) in 20 μl DB buffer (50 mmol/l NaCl, 300 mmol/l sucrose, 10 mmol/l PIPES, 3 mmol/l $MgCl_2 \cdot 6H_2O$, 1 mmol/l EGTA, pH 6.8) at 37 °C for 30 min, then 1 mol/l $(NH_4)_2SO_4$ was added at the final concentration of 0.25 mol/l and stored for 5 min. Finally, the copper net was washed three times (5 min each) with PBS (pH 7.2). Unless indicated otherwise all operations were performed at 4 °C [20]. The samples were fixed and dehydrated as described above, then dried in CO_2. Following this treatment, the structure of the nuclear matrix-lamina in the nuclei could be specifically restrained. The samples were observed and pictures were taken under JEM-1010 TEM.

Results

Induction of typical apoptotic morphological changes in CS-100. When incubated with the CS-100 induction system, the nuclei underwent a series of typical apoptotic changes. Chromatin condensation and margination could be seen after incubation for 1 h (fig. 1.2). After 2 h incubation, chromatin condensation had intensified and the chromatin shrank into blocks. These blocks were then extruded into the cytosol as apoptotic bodies (fig. 1.3). After 4 h incubation, intact nuclei could not be found in this apoptosis induction cocktail and high-fluorescent 'balls' filled the fluorescent microscope field (fig. 1.4). In control CS-100 without addition of cytochrome c, the nucleus remained intact during 4 h of incubation (fig. 1.1).

Typical apoptotic DNA degradation during the apoptosis of nuclei in the CS-100 induction system. A DNA ladder, the occurrence of specific DNA degradation into oligonucleosomal fragments, is a typical and symptomatic feature of cells undergoing apoptosis. The present results showed that a typical DNA ladder could be observed after the nuclei had been induced in the CS-100 induction system. Cytochrome c was added into the CS-100 cell-free system at a final concentration of 2 μmol/l. After induction for 0.5 h, only some of the DNA had been degraded. 1 h later, more DNA had been degraded and formed a DNA ladder. After 2 h, the ladder was more typical, i.e., most of the DNA was degraded into small fragments. For a CS-100 cell-free system without cytochrome c and for nuclei in the storage buffer with cytochrome c, there was no degradations of the total DNA after 4 h incubation (fig. 2).

Observation of apoptotic morphological changes by TEM. Samples of apoptotic nuclei in the CS-100 induction system were prepared at time intervals of 30 min, and then sections were made with the Leica Ultracut R cutter. Using JEM-1010 TEM, chromatin condensation and margination could be observed after nuclei had been incubated for 0.5 h, and this kind of change was synchronous in the nuclei undergoing apoptosis (fig. 3). During nuclear apoptosis, some small vesicles, which developed from the nuclear membrane and did not contain chromatin, were expelled from nuclei (fig. 3, arrows). Using TEM, we analyzed the details of apoptosis at different time intervals. In the initial phase (incubation for 0.5 h), chromatin condensation and margination could be observed. This kind of change accompanied the chromatin-free nuclear vesicles that were expelled from the nuclear membrane (fig. 4.2, arrows). After incubation for 1 h, 'large' vesicles, with blocks of condensed chromatin, were expelled from the nucleus (fig. 4.3, arrows). An enlarged view of the 'large' vesicle showed more clearly the small blocks of condensed chromatin accompanying the expelled vesicle

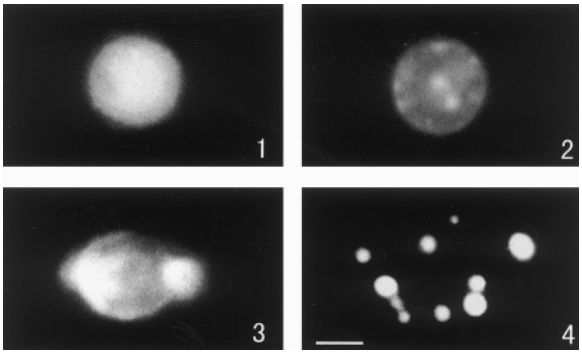

Figure 1. Observation of apoptotic nuclei in the CS-100 induction system using fluorescent microscopy (bar = 2 μm). (*1*) Negative control; the nucleus remained intact when stained with DAPI and observed under the microscope after incubation for 4 h at 23 °C in the CS-100 system without cytochrome c. (*2*) After incubation for 1 h in the CS-100 induction system, chromatin condensation and margination could be seen in the nucleus. (*3*) After 2 h, chromatin condensation has intensified and there is extrusion into the cytosol as apoptotic bodies. (*4*) After 4 h, the apoptotic nucleus has split into several apoptotic bodies.

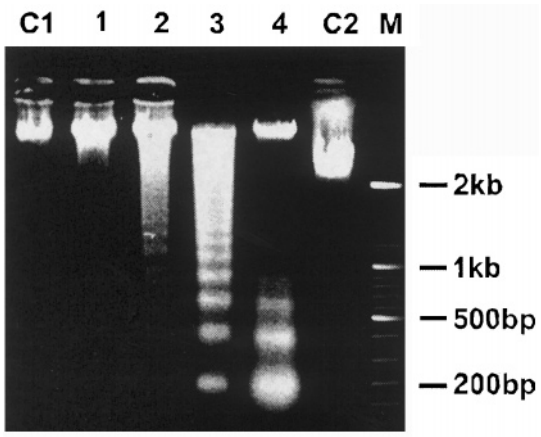

Figure 2. Specific degradation of DNA into oligonucleosomal fragments in the CS-100 induction system. Lane 1, after incubation for 0.5 h in the cell-free induction system, some of the DNA had been degraded. Lane 2, DNA was degraded into large fragments after incubation for 1 h, but no DNA ladder was seen. Lane 3, after 2 h incubation, DNA was more degraded, and a DNA ladder could be observed clearly. Lane 4, after 4 h incubation, the total DNA was degraded into small fragments, and the typical DNA ladder could be seen. Lane C_1, negative control, after incubation for 4 h in the CS-100 cell-free system without cytochrome c; total DNA of nuclei was not degraded. Lane C_2, control, nuclei were added to storage buffer with cytochrome c: after incubation for 4 h, there was no degradations of total DNA. Lane M, DNA molecular-weight marker (Boehringer Mannheim).

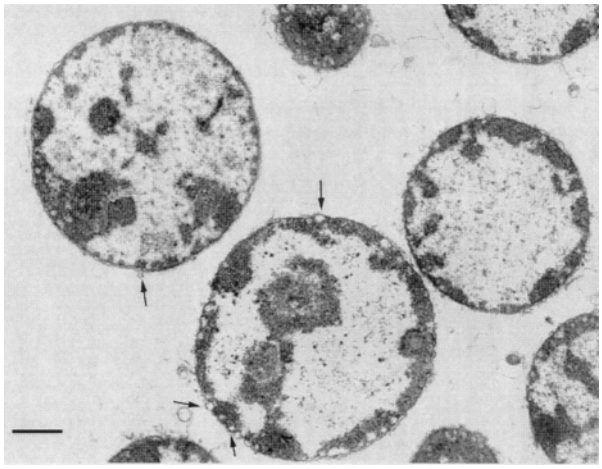

Figure 3. Ultrastructural sections showing chromatin condensation and margination of apoptotic nuclei incubated for 0.5 h in the cell-free induction system. The morphological changes in apoptotic nuclei were synchronous. Some chromatin-free nuclear vesicles, which evolved from the nuclear membrane and had no chromatin, were expelled from apoptotic nuclei (arrows). Bar = 1 μm.

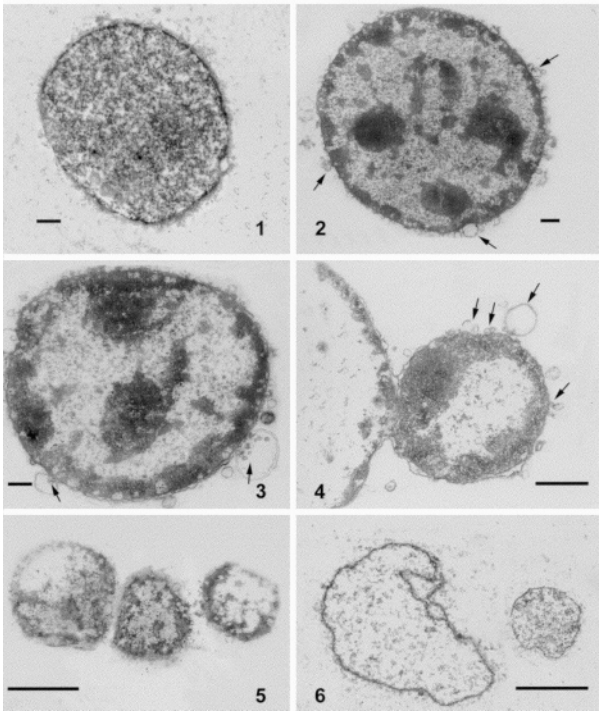

Figure 4. Nuclear apoptotic process in a cell-free induction system. Bar = 1 μm. (*1*) Negative control. After incubation for 4 h in the cell-free system without cytochrome c, the nuclear chromatin remained intact. (*2*) After incubation for 0.5 h in the CS-100 induction system, the chromatin in the nucleus underwent condensation and margination and chromatin-free nuclear vesicles expelled (arrows). (*3*) After incubation for 1 h, 'large' vesicles, with a small amount of condensed chromatin were expelled from the nucleus (arrows). (*4*) After 2 h, an apoptotic body containing condensed chromatin is seen being expelled from the nucleus. There are chromatin-free nuclear vesicles on the surface of the apoptotic body (arrows). (*5*) After 4 h, the apoptotic nucleus has split into several apoptotic bodies. (*6*) At the same time, the residual nucleus can be seen without chromatin.

(fig. 5, arrows). At the anaphase of apoptosis (incubation for 2 h), the apoptotic body was being expelled from the nucleus and contained much condensed chromatin (fig. 4.4). At the telophase of apoptosis, the nucleus could no longer maintain its structure and the apoptotic nucleus was split into several apoptotic bodies (fig. 4.5/6). After 4 h incubation, chromatin in the nucleus added into the cell-free system without cytochrome c remained intact (fig. 4.1). After incubation for 1 h with Ac-YVAD-CHO, chromatin condensation and margination could be observed, but no vesicles were observed on the surface of the nucleus (fig. 6).

Observation of apoptotic bodies using SEM. SEM results showed that apoptotic bodies were expelled from the nucleus (fig. 7), together with chromatin-free nuclear vesicles. Nuclear pore complex-like structures could be seen clearly on the surface of the nucleus, but not on the surface of apoptotic bodies.

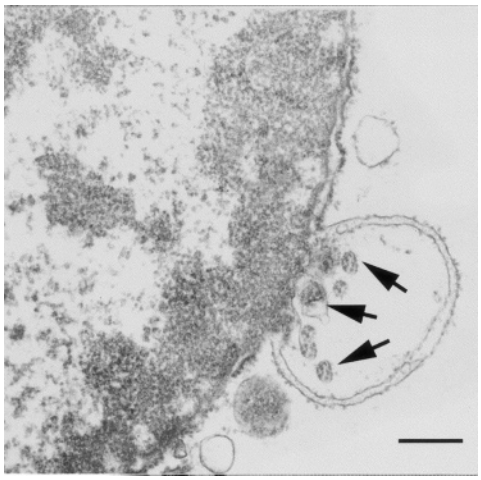

Figure 5. Enlargement of figure 4.3, a 'large' vesicle being expelled from the nucleus. The membranes of these vesicles were also bilayer. The arrows indicate condensed small chromatin blocks transposed into the vesicle. Bar = 0.3 μm.

Observation of apoptotic nuclei using whole-mount electron microscopy. The results from whole-mount electron microscopy indicated that the lamina structure of the nucleus was destroyed during the apoptotic process of nuclei in the CS-100 induction system. This change was accompanied by the evolution of apoptotic bodies.

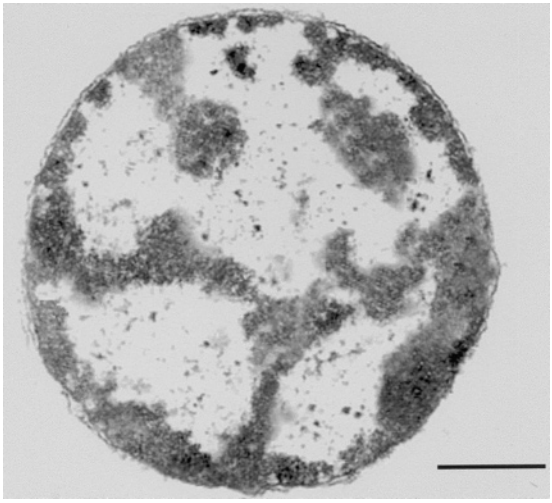

Figure 6. Influence of Ac-YVAD-CHO on vesicle appearance. After addition of 5 μmol/l Ac-YVAD-CHO into the cell-free induction system and incubation at 23 °C for 1 h, the TEM picture showed that the chromatin in the nucleus had undergone condensation and margination. However, there were no chromatin-free nuclear vesicles on the surface of the apoptotic nucleus. Bar = 1 μm.

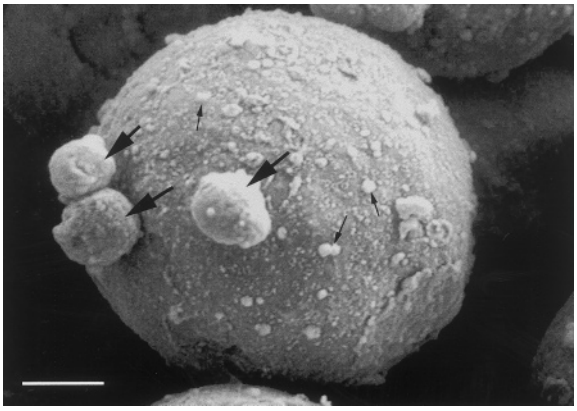

Figure 7. Observation of apoptotic bodies using SEM. After incubation for 2 h in the cell-free induction system, apoptotic bodies (large arrows) are seen being expelled from the nucleus. The small arrows indicate chromatin-free nuclear vesicles. Bar = 1 μm.

The results also showed that the apoptotic body was connected with the nucleus through the nuclear matrix (fig. 8.1). At the telophase (incubation for 4 h in the cell-free induction system), lamins were completely degraded; however, although the nuclear matrix was greatly damaged, its network structure persisted and formed the structural basis of the apoptotic body (fig. 8.3). When Ac-YVAD-CHO was added to the induction system, the lamina structure remained intact, while the nuclear matrix structure was partly destroyed after incubation for 2 h at 23 °C (fig. 8.2). However, the nuclear matrix-lamina structure remained integrated in the control group, in which the nuclei were incubated at 23 °C for 4 h in the CS-100 cell-free system without cytochrome c (fig. 8.4).

Discussion

Specific morphological changes, such as chromatin condensation, margination, and formation of apoptotic bodies, are important features of cells undergoing apoptosis [2, 3, 13]. Lamin degradation occurs before the morphological changes of apoptosis and seems to be the foundation of the morphological changes. Since there are no other organelles in the cell-free system but nuclei, the apoptotic morphological changes of the nucleus are important indications of apoptosis. Furthermore, it is quite helpful to study apoptosis in a cell-free system, because the morphological and structural changes can be observed directly, avoiding artifacts that may arise when isolating nuclei from apoptotic cells.

Selective extraction, first developed in the laboratory of Penman [23], was useful for studying the structure of

the nuclear matrix-lamina system. In living cells, this system, comprising lamins and other nonhistones, supports the normal conformation of the nucleus and plays an important role in cell function [24, 25]. The lamina under the nuclear membrane is constructed by three kinds of lamins, lamin A, B, and C [8]. In a normal nucleus, chromosomes are specifically connected with the lamina through their telomeres [9–11]. However, what happens to this structural system during the apoptotic process is still unclear. The morphological changes related to the degradation of lamins beneath the nuclear membrane are important characteristics of apoptosis. The degradation of lamin proteins leads to a series of typical apoptotic morphological changes [6]. During apoptotic progression, caspase 6, activated by caspase 3, has been proposed to contribute to the degradation of lamins and its activity can be inhibited by Ac-YVAD-CHO [26]. However, in the CS-100 cell-free system, Ac-YVAD-CHO can also inhibit formation of the DNA ladder [18]. In mammalian cells, caspase 3 degrades ICAD [DFF45, an inhibitor of caspase-activated DNase (CAD)] to free CAD (DFF40). Activated CAD specifically cuts the chromatin into a DNA ladder between the nucleosomes [27, 28]. Degradation of lamins and DNA follow a parallel time course [12]. However, the relationships among the typical morphological features of apoptosis still remain unclear, including the degradation of lamins, the specific degradation of DNA, and the formation of apoptotic bodies. Using TEM, SEM, and whole-mount electron microscopy, we observed details of the morphological changes during the apoptotic process. Combining the results of the degradation of DNA and lamins (Western blot) [18] with the alterations in the nuclear matrix-lamina structure system, we can sketch a map of the mechanism of apoptotic body formation.

The relationship between specific degradation of DNA and the formation of apoptotic bodies. CS-100 is a good cell-free system for studying the apoptotic mechanism [16–18]. We succeeded in reconstructing nuclei in the system [19], and have shown that nuclei from either animals or plants can be effectively triggered into apoptosis [17, 18], even though the system is from the cytosol of carrot cells. We hope that the CS-100 will be a powerful tool for studying evolutionary relationships between plants and other species. There appears to be phylogenetic conservation not only of the apoptotic pathway leading to nuclear changes but also of caspase-like proteins. Stained with DAPI, the typical apoptotic morphological changes of nuclei undergoing apoptosis after induction in the CS-100 system by cytochrome c could be observed using a Leica DMRB fluorescent

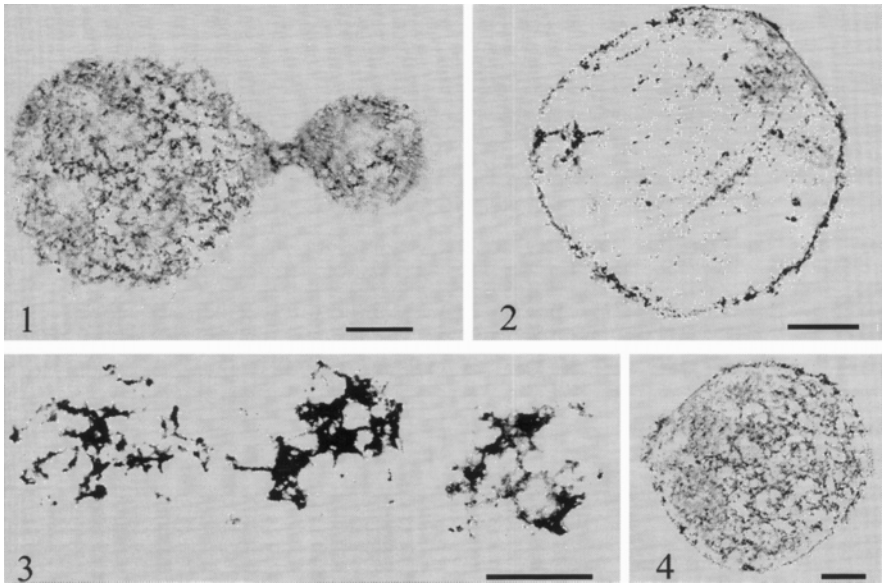

Figure 8. Observation of an apoptotic nucleus using whole-mount electron microscopy. Bar = 1 μm. (*1*) After incubation for 2 h in the apoptosis induction system, the lamina structure of the apoptotic nucleus had been destroyed. The apoptotic body was connected with the nucleus through the nuclear matrix. (*2*) After 5 μmol/l Ac-YVAD-CHO had been introduced into the cell-free induction system, the lamina system of the nucleus remained intact in nuclei induced to undergo apoptosis for 2 h by cytochrome c. However, most of the nuclear matrix seemed to be destroyed. (*3*) After incubation for 4 h, most of the nuclear matrix structure was visible and still formed the structural foundation of the apoptotic body. (*4*) Negative control, after incubation for 4 h in the CS-100 system without cytochrome c; the nuclear matrix-lamina system remained intact.

microscope. After chromatin condensation, the formation of apoptotic bodies could also be observed (fig. 1). The TEM results suggested that nuclei underwent apoptosis with high synchronization in the CS-100 cell-free induction system (fig. 3).

As described above, in the initial phase of apoptosis (incubation for 0.5 h in the CS-100 induction system), the DNA of apoptotic nuclei became partially degraded (fig. 2.1). At the same time, morphological evidence (figs 1.2, 3, and 4.2) indicated that chromatin condensation and margination began to occur and were accompanied by expulsion of chromatin-free nuclear vesicles from the surface of nuclei (figs 3, 4.2). The partial degradation of the DNA contributed to the formation of the large DNA fragments. Since chromatins are connected to the lamina by telomeres, the ruptured chromatin DNA was dragged to the telomeres where it condensed and became marginated. Because chromatin DNA was only degraded into large fragments, no chromatin appeared in the nuclear vesicles being expelled from the nucleus.

At the metaphase of apoptosis (incubation for 1 h in the CS-100 induction system), electrophoretic analysis revealed DNA fragments (of about 1 kb) but no DNA ladder (fig. 2.2). TEM results suggested there were more chromatin-free nuclear vesicles on the surface of the apoptotic nucleus than in the initial phase, some of which were quite large. In addition, a few small chromatin blocks were found in some large vesicles (figs 4.3, 5), the activated CAD having made more cuts in the chromatin, so that small pieces of DNA could now be expelled from the nucleus.

At the anaphase of apoptosis (incubation for 2 h), chromatin DNA had been sufficiently degraded to form a DNA ladder (fig. 2.3). The DNA fragments were expelled from the nucleus together with the apoptotic body (figs 1.3, 4.4).

At the telophase of apoptosis (incubation for 4 h), chromatin DNA had been further degraded (fig. 2.4). The apoptotic nucleus could no longer maintain its integrity and evolved into several apoptotic bodies and a residual anomalous nuclear membrane structure, in which there was no chromatin (figs 4.5, 4.6).

The relationship between specific degradation of lamins and the formation of the apoptotic body. In the apoptotic process, lamins are specially degraded by caspase 6, activated by caspase 3 [26]. Our experimental results suggested that at the initial phase of apoptosis (incubation for 0.5 h), when 64-kDa lamin is first degraded [18] (see fig. 9), the typical apoptotic changes begin; including chromatin condensation and margination (figs 1.2, 3, and 4.2), and the formation of the chromatin-free nuclear vesicles on the nuclear surface. Degradation of 64-kDa lamin could lead to the formation of these chromatin-free nuclear vesicles, enveloped by the nuclear membrane.

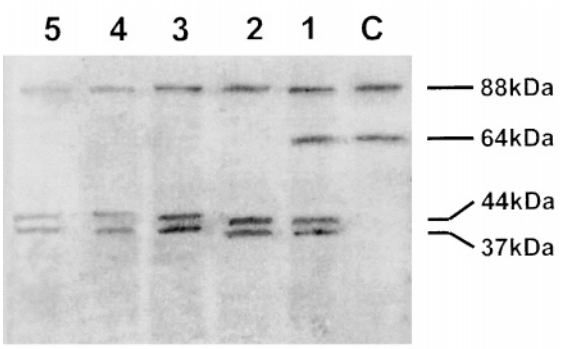

Figure 9. Western blot showing the specific degradation of lamin proteins during apoptosis of nuclei. Lane C, negative control: lamin proteins remained intact after 4 h incubation in the CS-100 cell-free system without cytochrome c; lane 1, incubation for 0.5 h in the cell-free induction system: 64-kDa lamin begins to show degradation into 44-kDa and 37-kDa fragments; lane 2, after incubation for 1 h: more lamins are degraded and 64-kDa lamin is no longer detectable; lane 3, after incubation for 2 h: decrease in 88-kDa lamin now clearly observable; lanes 4, 5, after incubation for 4 and 8 h, respectively: gradual disappearance of lamin proteins and their degradation products [from ref. 19 with permission].

At the metaphase of apoptosis (incubation for 1 h), 64-kDa lamin was more intensively but not completely degraded [18]. This degradation was accompanied by lamina was destruction, giving rise to the large and chromatin-free nuclear vesicles (figs 4.3, 5). The formation of these vesicles could be inhibited by the caspase inhibitor, Ac-YVAD-CHO (fig. 6).

At the anaphase of apoptosis (incubation for 2 h), 64-kDa lamin was degraded completely and 88-kDa lamin began to show signs of digestion [18]. These changes contributed to complete break down of the lamina in the nucleus and apoptotic body expulsion. At the same time, there were still some chromatin-free nuclear vesicles on the surface of the apoptotic body (fig. 4.4). Whole-mount electron microscopy results suggested that there was only residual nuclear matrix in the apoptotic body and the lamina of the nucleus was completely destroyed. Nuclear matrix connected the apoptotic body with the nucleus (fig. 8.2) and formed the structural foundation of the apoptotic body. However, when Ac-YVAD-CHO was introduced into the cell-free induction system, destruction of the lamina system and appearance of apoptotic bodies were inhibited (fig. 8.4). SEM results also showed the evolution of apoptotic bodies when nuclei were incubated for 2 h in the CS-100 cell-free induction system (fig. 7). Nuclear pore complex-like structures were clearly observed on the surface of the nucleus, where there were no vesicles expelled. But no such structures were seen on the sur-

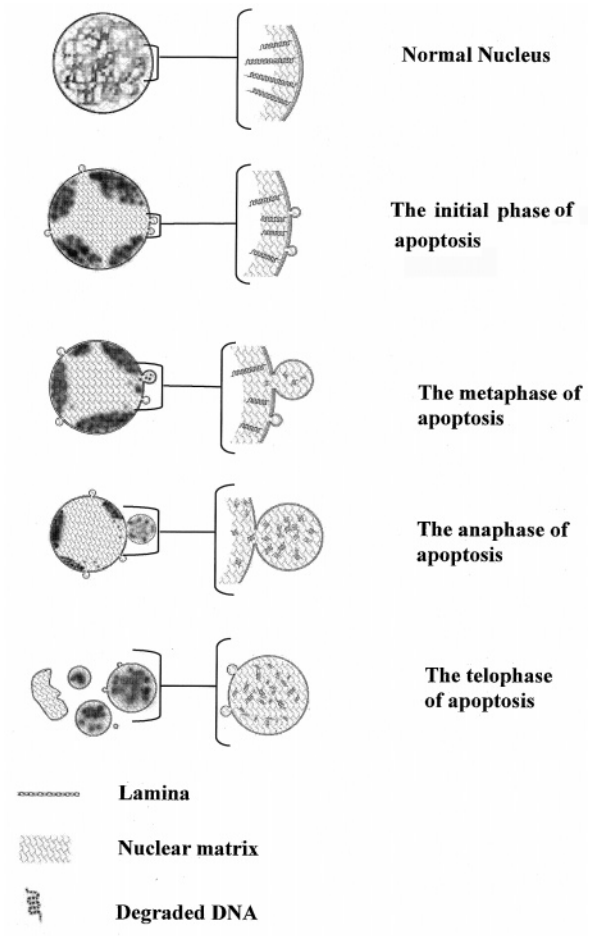

Figure 10. A schematized diagram showing the apoptotic process of the nucleus.

face of apoptotic bodies. This also suggested that various changes in protein conformational structure had occurred in the nucleus, either to nuclear membrane proteins or due to destruction of the lamina.

Thus, complete degradation of 64-kDa lamin and partial degradation of 88-kDa lamin were responsible for the drastic destruction of the lamina system. At the same time, chromatin DNA was specifically degraded by activated CAD and was cut between the nucleosomes to form the DNA ladder. The nuclear matrix evolved into the apoptotic body, and the condensed chromatin was expelled from nucleus with the apoptotic body.

At the telophase of apoptosis (incubation for 4 h), nuclear lamins were almost completely degraded [18]. The apoptotic nucleus could not maintain its integrity, and evolved into several apoptotic bodies and a residual anomalous nuclear membrane structure, in which there was no chromatin (figs 4.5, 4.6). There was a residual nuclear matrix system in the apoptotic bodies and formed the structural network for the apoptotic bodies (fig. 8.3).

The entire apoptotic process of the nucleus is schematized in figure 10. Some chromatin-free nuclear vesicles, in which there is no chromatin, formed before the evolution of apoptotic bodies; apoptotic body formation occurs at a comparatively late phase, and they contain much chromatin. Nuclear matrix connects the apoptotic bodies with the apoptotic nucleus and provides the structural foundation of the apoptotic bodies.

Acknowledgements. We are indebted to Dr. Junying Yuan, assistant professor of Harvard Medical School, for her careful reading and criticism of the manuscript. This work was supported by grants from the Chinese National Foundation of Natural Sciences (grant numbers 39800075 and 19890380) and Projects Under the Major State Basic Research Program of P. R. China (grant number G1999053905).

1 Steller H. (1995) Mechanisms and genes of cellular suicide. Science **267:** 1445–1449
2 Nagata S. (1997) Apoptosis by death factor. Cell **88:** 355–365
3 Wyllie A. H. (1980) Glucocorticoid-induced thymocyte apoptosis is associated with endogenous endonuclease activation. Nature **284:** 555–556
4 Liu X., Kim C. N., Yang J., Jemmerson R. and Wang X. (1996) Induction of apoptotic program in cell-free extracts: requirement for dATP and cytochrome c. Cell **86:** 147–157
5 Tang D. G., Li L., Zhu Z. and Joshi B. (1998) Apoptosis in the absence of cytochrome c accumulation in the cytosol. Biochem. Biophys. Res. Commun. **242:** 380–384
6 Neamati N., Fernandez A., Wright S., Kiefer J. and McConkey D. J. (1995) Degradation of lamin B1 precedes oligonucleosomal DNA fragmentation in apoptotic thymocytes and isolated thymocyte nuclei. J. Immunol. **154:** 3788–3795
7 Ludérus M. E., van Steensel B., Chong L., Sibon O. C., Cremers F. F. and de Lange T. (1996) Structure, subnuclear distribution, and nuclear matrix association of the mammalian telomeric complex. J. Cell Biol. **135:** 867–881
8 Gerace L., Comeau C. and Benson M. (1984) Organization and modulation of nuclear lamina structure. J. Cell Sci. Suppl. **1:** 137–160
9 Wang G. S., Luo W. J., Pan W. J., Ding M. X. and Zhai Z. H. (1994) Association of chromosomal telomere DNA with nuclear matrix in Hela cell. Sci. China **37**(6)**:** 691–699
10 Wang G. S., Luo WJ, Ding M. X. and Zhai Z. H. (1993) Relation between localization of chromosomal telomere and nuclear matrix-lamina of Hela cell. Chin. Sci. Bull. **38:** 1295–1299
11 Amati B. B. and Gasser S. M. (1988) Chromosomal ARS and CEN elements bind specifically to the yeast nuclear scaffold. Cell **54:** 967–978
12 Lazebnik Y. A., Takahashi A., Moir R. D., Goldman R. D., Poirier G. G., Kaufmann S. H. et al. (1995) Studies of the lamin proteinase reveal multiple parallel biochemical pathways during apoptotic execution. Proc. Natl. Acad. Sci. USA **92:** 9042–9046
13 Zhang J., Reedy M. C., Hannun Y. A. and Obeid L. M. (1999) Inhibition of caspases inhibits the release of apoptotic bodies: Bcl-2 inhibits the initiation of formation of apoptotic bodies in chemotherapeutic agent-induced apoptosis. J. Cell Biol. **145:** 99–108
14 Lazebnik Y. A., Cole S., Cooke C. A., Nelson W. G. and Earnshaw W. C. (1993) Nuclear events of apoptosis in vitro in

cell-free mitotic extracts: a model system for analysis of the active phase of apoptosis. J. Cell Biol. **123:** 7–22
15 Juin P., Pelletier M., Oliver L., Tremblais K., Grégoire M., Meflah K. et al. (1998) Induction of a caspase-3-like activity by calcium in normal cytosolic extracts triggers nuclear apoptosis in a cell-free system. J. Biol. Chem. **273:** 17559–17564
16 Luo X., Budihardjo I., Zou H., Slaughter C. and Wang X. (1998) Bid, a Bcl2 interacting protein, mediates cytochrome c release from mitochondria in response to activation of cell surface death receptors. Cell **94:** 481–490
17 Zhao Y., Sun Y. L., Jiang Z. F. and Zhai Z. H. (1999) Apoptosis of carrot nuclei in in vitro system induced by cytochrome c. Chin. Sci. Bull. **44:** 1497–1501
18 Zhao Y., Jiang Z. F., Sun Y. L. and Zhai Z. H. (1999) Apoptosis of mouse liver nuclei induced in the cytosol of carrot cells. FEBS Lett. **448:** 197–200
19 Zhao Y., Liu X. L., Wu M., Tao W. and Zhai Z. H. (2000) In vitro nuclear reconstitution could be induced in a plant cell-free system. FEBS Lett. **480:** 208–212
20 Yang J., Bhalla K., Kim C. N., Ibrado A. M., Peng T. I., Jones D. P. et al. (1997) Prevention of apoptosis by Bcl-2: release of cytochrome c from mitochondria blocked. Science **275:** 1129–1132
21 Kluck R. M., Bossy-Wetzel E., Greene D. R. and Newmeyer D. W. (1997) The release of cytochrome c from mitochondria: a primary site of Bcl-2 regulation of apoptosis. Science **275:** 1132–1136
22 Blobel G. and Potter U. R. (1966) Nuclei from rat liver: isolation method that combines purity with high yield. Science **154:** 1662–1665
23 Capco D. G., Krochmalnic G. and Penman S. (1984) A new method of preparing embeddment-free sections for transmission electron microscopy: applications to the cytoskeletal framework and other three-dimensional networks. J. Cell Biol. **98:** 1878–1885
24 Hakes D. J. and Berezney R. (1991) DNA binding properties of the nuclear matrix and individual nuclear matrix proteins: evidence for salt-resistant DNA binding sites. J. Biol. Chem. **266:** 11131–11140
25 Tawfic S., Faust R. A., Gapany M. and Ahmed K. (1996) Nuclear matrix as an anchor for protein kinase CK2 nuclear signaling. J. Cell Biochem. **62:** 165–171
26 Takahashi A., Alnemri E. S., Lazebnik Y. A., Fernandes A. T., Litwack G., Moir R. D. et al. (1996) Cleavage of lamin A by Mch2 alpha but not CPP32: multiple interleukin 1 beta-converting enzyme-related proteases with distinct substrate recognition properties are active in apoptosis. Proc. Natl. Acad. Sci. USA **93:** 8395–8400
27 Tang D. and Kidd V. J. (1998) Cleavage of DFF-45/ICAD by multiple caspases is essential for its function during apoptosis. J. Biol. Chem. **273:** 28549–28552
28 Inohara N., Koseki T., Chen S., Benedict M. A. and Nunez G. (1999) Identification of regulatory and catalytic domains in the apoptosis nuclease DFF40/CAD. J. Biol. Chem. **274:** 270–274